A versatile living polymerization method for aromatic amides

Subhajit Pal,[1] Dinh Phuong Trinh Nguyen, [1] Angélique Molliet, [1] Mahshid Alizadeh, [1] Aurélien Crochet, [1] Roberto D. Ortuso,[2] Alke Petri-Fink[1,2] and Andreas F.M. Kilbinger[1]*

[1] Department of Chemistry, University of Fribourg, Chemin du Musée 9, CH-1700 Fribourg, Switzerland.
[2] Adolphe Merkle Institute, University of Fribourg, Chemin des Verdiers 4, CH-1700 Fribourg, Switzerland.
* andreas.kilbinger@unifr.ch

Abstract

Polycondensation polymers typically follow step growth kinetics assuming all functional groups are equally likely to react with one another. If the reaction rates with the chain end can be selectively accelerated, living polymers can be obtained. Here, we report on two chlorophosphonium iodide reagents that have been synthesized from triphenylphosphine and tri(*o*-methoxyphenyl)phosphine. The former activates aromatic carboxylic acids as acid chlorides in the presence of secondary aromatic amines and the latter even in the presence of primary aromatic amines. These reagents allow *p*-aminobenzoic acid derivatives to form solution stable activated monomers that polymerize in a living fashion in the presence of amine initiators. Other aryl amino acids and even dimers of aryl amino acids can be polymerized in a living fashion when slowly added to the phosphonium salt in the presence of an amine initiator. Diblock copolymers as well as a triblock terpolymer of aryl amino acids could be prepared even in the presence of electrophilic functional groups.

Many industrially important polymers such as polyesters, polyamides or polyurethanes follow step growth kinetics in which the monomer, oligomer and polymer end groups can all react with one another. As was shown early on by Carothers,[1] high extends of reaction (conversion) are needed for such reactions to achieve high molecular weight polymers. However, all step-growth polymerizations approach a dispersity of Đ=2.0 for high extends of reaction (conversion) and the synthesis of step-growth block copolymers is not possible out of principle. Many naturally occurring macromolecules, such as proteins or nucleic acids can formally be classified as condensation polymers. While typical synthetic condensation polymers such as polyesters or polyamides follow step growth kinetics with the limitations mentioned above, nucleic acids and proteins have discrete molecular masses and are precisely monomer sequence controlled. With these examples, nature beautifully illustrates how high levels of sequence control directly result in regulation of the supramolecular structure, aggregation and, ultimately, chemical function.

It is, therefore, not surprising that chemists have been trying to mimic nature with varying degrees of polymerization control. Several synthetic routes have been explored to gain control over the monomer sequence for synthetically prepared oligomers and short polymers. Merrifield's peptide synthesis[2,3,4] is one of the best known synthetic approaches representing an organic chemistry step wise procedure on a solid support. Most recently, much progress has been made in polymeric approaches to gain sequence control[5,6,7,8,9,10]. However, the number of monomers that can be precisely arranged in Merrifield's solid phase synthesis is still out of reach for polymer synthesis.

The limitation of broad dispersities for condensation polymers could be overcome for several types of monomers[11,12,13] as was shown by Yokozawa et al. The basic principle behind Yokozawa's innovative approach was the self-deactivation of condensation monomers, thereby

preventing classical step-growth kinetics. The polymers obtained by this elegant method showed narrow dispersity and the possibility to form block copolymers.
Poly(aromatic amides) are amongst the best investigated polymers in this context. However, low temperatures, the use of strong bases and several known side reactions[14] limit this technique as far as the average molar mass of the polymers is concerned (Mn=22 kDa).[15] As strong nucleophiles are required throughout the polymerization, the method is limited to monomers devoid of electrophilic functional groups.
In particular, this technique could not yet be applied to the growing field of aromatic amide foldamers which aims at mimicking the function of biological macromolecules with similarly sized synthetic oligo and polyamides.[16,17,18,19,20,21,22,23,24]
Here, we present a more versatile living polymerization method for monomeric or oligomeric aromatic amino acids, irrespective of their potential for self-deactivation. The method is based on the fast and selective formation of aromatic acid chlorides in the presence of aromatic amines. This allows for a chain growth polymerization mechanism either by monomer self-deactivation or via slow monomer addition.

Results and Discussion

Reagent screening

Yokozawa's living polycondensation method relies on the self-deactivation of para- or meta-substituted aminobenzoic acid monomers whereby the amide anion acts as a strongly electron donating group which renders the carboxylic ester in para or meta position less electrophilic. This means that the polymerization via self-initiation is insignificant on the timescale of the initiated propagation reaction. In this way, monomers would only react with an initiator, or later with the growing polymer chain end. As a result, classical step growth monomers mimic chain growth kinetics.
We were curious as to whether monomers with reversed polarity, i.e. carrying a free amine in para-position of an acid chloride, would show identical self-deactivation behavior. If successful, a larger monomer pool carrying various electrophilic functional groups, such as amides or esters, could be made available for such a living polymerization method. Unfortunately, acid chloride activation protocols that tolerate the presence of primary or secondary aromatic amines are scarce[25,26,27] and often not suitable for the synthesis of aromatic amides. While investigating triphenyl phosphonium activating agents for aromatic carboxylic acids, we discovered that triphenyl phosphine (Ph_3P) activated by iodine chloride (ICl) resulted in a soluble (dichloromethane, DCM) reagent that cleanly converted carboxylic acids into the corresponding acid chlorides under very mild reaction conditions[28,29] (Supplementary Scheme 1 and Supplementary Fig. 3, 18). Moreover, it tolerated the presence of secondary aromatic amines (Supplementary Fig. 11, 12).
This behavior is unusual because a similar reagent prepared from Ph_3P/I_2 does not activate carboxylic acids and is poorly soluble in DCM, whereas the analogous Ph_3P/Cl_2 activates carboxylic acids, reversibly reacts with aromatic amides (Supplementary Fig. 5, 6) but irreversibly reacts with secondary aromatic amines (Supplementary Fig. 1, 2, 8-10).
Furthermore, we observed that aliphatic alcohols react with Ph_3P/ICl (**PHOS1**) to give aliphatic iodides exclusively (Supplementary Scheme 1 and Supplementary Fig. 24). The x-ray crystal structure of **PHOS1** shows a disordered arrangement in which both, iodine and chlorine, are bound to the phosphorous atom with either an iodide or chloride counter ion (Fig. 1 and Supplementary Fig. 103, 104). ^{31}P-NMR spectroscopy in DCM-d_2, however, showed that, in addition to small amounts of triphenylphosphineoxide from hydrolysis due to water impurities, only one major species was present in solution (δ 65 ppm) which appeared to be in equilibrium with a non-ionic species in the presence of iodide and chloride ions (Supplementary Fig. 3, 23, 94). We propose that initially, Ph_3P reacts with ICl in DCM to form

the iodophosphonium chloride in which the highly nucleophilic chloride anion substitutes the iodide to form the chlorophosphonium iodide as the major species in solution (Supplementary Scheme 1).[30] We believe that the presence of this species is responsible for the exclusive formation of aliphatic iodides from alcohols via an intermediate pentavalent alkoxide adduct in which the iodide counter ion is the only nucleophile present for aliphatic nucleophilic substitution (Supplementary Scheme 1 and Supplementary Fig. 24-26). Furthermore, the ^{31}P-NMR shift of the phosphorous signal of **PHOS1** (DCM-d_2, δ=65.7) is in agreement with an ionic chlorophosphonium species (Ph_3P/Cl_2: δ =58.6).[31,32,33] In the case of carboxylic acid activation, we can only speculate that an intermediate carboxylic acid iodide[34,35] might be formed and immediately converts into the carboxylic acid chloride. However, mechanistically we cannot distinguish this scenario from one where the acid chloride is formed directly.
It is, however, worth emphasizing at this point that the mere exchange of the counter ion of the chlorophosphonium cation from chloride (as in Ph_3P/Cl_2) to iodide has a dramatic effect on the reactivity and in particular the tolerance of the reagent towards secondary amines.

Polymerizations of N-alkylated aromatic amino acids
Next, we evaluated **PHOS1** in a polymerization with a potentially self-deactivated monomer following Yokozawa's method but with reversed monomer polarity. We therefore added a DCM solution of monomer *N*-ethylhexyl-4-aminobenzoic acid (**A**, Fig. 1) and initiator *N*-methyl-4-bromo-aniline (**I1**) to a cooled (0°C) DCM solution of **PHOS1**. After stirring at 0°C for 30 min. pyridine was added to the mixture and the reaction was allowed to warm to rt. Intermittent ^{1}H-NMR spectroscopic analysis of crude reaction samples allowed us to follow the progression of the polymerization (Supplementary Fig. 30). After 16h, the reaction was terminated by the addition of water and the polymer (**PA1**) was isolated and analyzed. The number average molar mass of the polymer obtained by size exclusion chromatography (SEC, THF, Mn=3700 g mol^{-1}) was close to the value determined by the [**A**]:[**I1**] ratio with a dispersity of Đ=1.1. Further polymerizations (**PA2**-**PA4**) using the same monomer (**A**) and initiator (**I1**) showed a linear relationship between the apparent molar mass (SEC, THF) and the varying [**A**]:[**I1**] ratio with dispersities around Đ=1.1 (Fig. 2a). To further investigate the polymerization kinetics, samples were taken from the polymerization to form **PA2** from monomer **A** and initiator **I1**. The molar mass of all samples was determined by GPC (THF) and the monomer conversion calculated from ^{1}H-NMR spectra (Supplementary Fig. 35, 187-193 and Supplementary Table 2). As shown in Fig. 2e (and Supplementary Fig. 34), a linear relationship between monomer conversion (up to 96%) and molar mass was observed. This is clear evidence that the polymers were formed in a living chain growth polymerization and a strong indication that the amino-acid chloride monomer was self-deactivated under these reaction conditions.
We then investigated the initiator methyl 4-aminobenzoate (**I2**) carrying a primary amine and a methyl ester in a polymerization with monomer **A**. The polymer obtained (**PA5**, Mn=5500 g mol^{-1}, Đ=1.1) showed narrow dispersity and a number average molar mass close to the target set via the [**A**]:[**I2**] ratio (Supplementary Table 1). Polymerization of **A** with initiator phenyl 4-((2,4-dimethoxybenzyl)amino)benzoate (**I3**) also fulfilled the criteria of a living polymerization (**PA6**, Mn=9200 g mol^{-1}, Đ=1.1). After purification by recycling SEC in $CHCl_3$, **PA2**, **PA5** and **PA6** could be analyzed by MALDI ToF mass spectrometry (Supplementary Fig. 109-111). The monoisotopic mass signals of the isotopically resolved polymer mass distributions matched the proposed structures (Supplementary Fig. 109-111) carrying the respective initiator fragments at one of the chain ends.
It is worth noting here, that our polymerization technique allows the presence of an ester group within the initiator structure. All previous reports of living aramide polymerization required

strong bases/nucleophiles and did, therefore, not tolerate reactive electrophiles within the initiator or monomer structure.
Furthermore, ^{1}H-NMR spectroscopic signal integration allowed the distinction between end group signals vs. monomer repeat units thereby providing an alternative method to determine the number average molar mass. The number average molar masses obtained in this way were in very good agreement with the target values (Supplementary Tables 1, 3, 4).

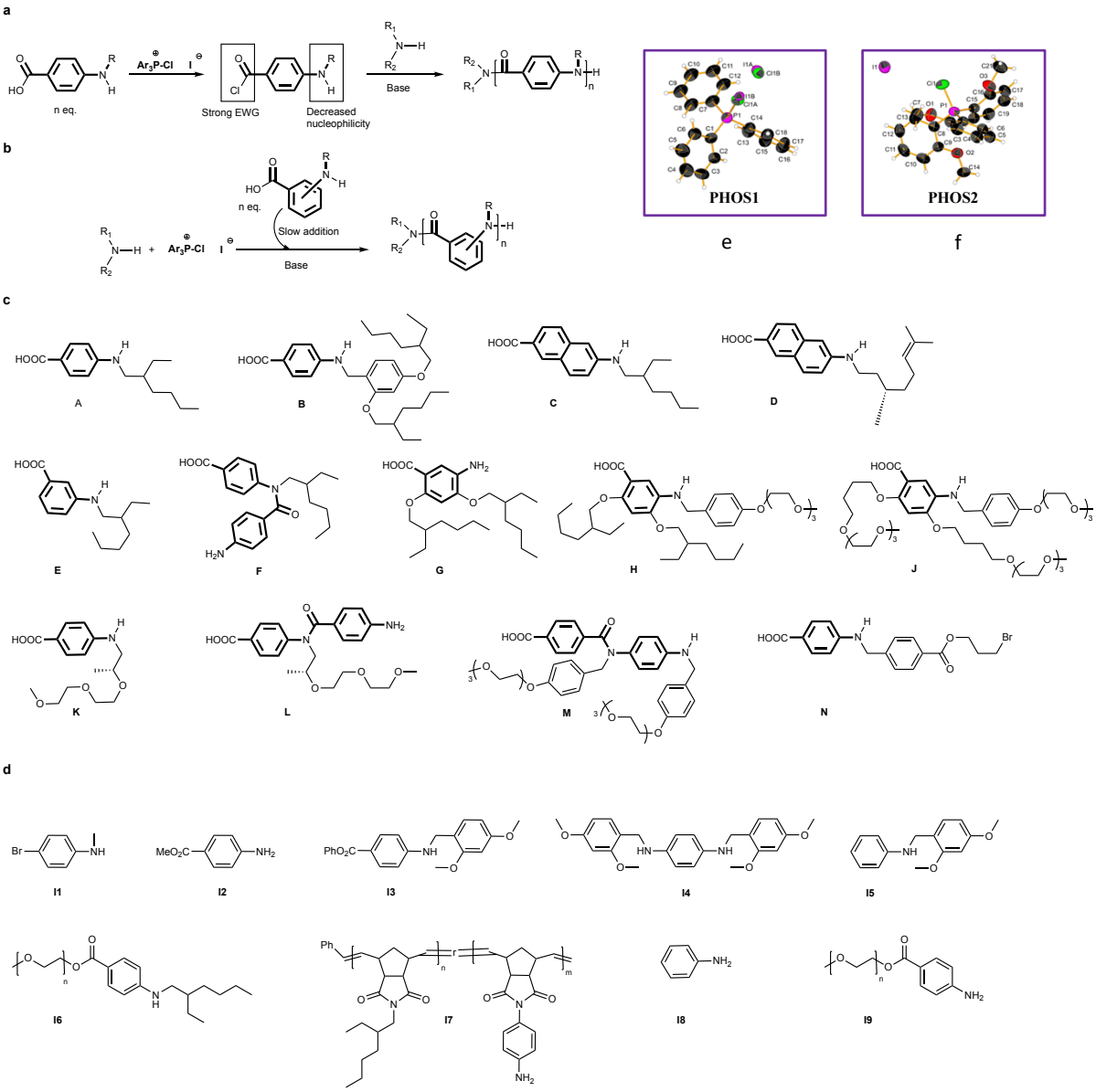

Fig. 1 Living polymerization of aromatic amino acids. **a**, One-pot polymerization method for self-deactivated *p*-aminobenzoyl chlorides. **b**, Slow monomer addition polymerization for non-self-deactivating *m/p*-aminobenzoyl chlorides. The active monomer is generated *in-situ* via slow addition, thereby avoiding bi-molecular step-growth side reactions. **c**, Structures of all monomers (**A**-**N**) and **d**, structures of all initiators (**I1**-**I9**) used in this study. **e**,**f**, X-ray crystal single structures of **PHOS1** and **PHOS2**.

Two further polymerizations were carried out using *para*-substituted and self-deactivating amino acid monomers. In the first case, a bifunctional initiator *N*,*N*′-bis(2,4-dimethoxybenzyl)phenylene diamine (**I4**) was used to polymerize monomer **A** (**PA7**,

Mn=28000 g mol $^{-1}$, Đ=1.1). In the other case, a monofunctional aniline initiator *N*-(2,4-dimethoxybenzyl)aniline (**I5**) was employed for the polymerization of 4-((2, 4-bis((2-ethylhexyl)oxy)benzyl)amino)benzoic acid (monomer **B**, Fig. 1) to give polymer **PB1** (Mn=8800 g mol^{-1}, Đ=1.1). A 200mer was targeted for **PA7** by adjusting the [**A**]:[**I4**] ratio accordingly. Even though **PA7** formed a clear dichloromethane solution, filtration through a 0.45µm pore size syringe filter proved difficult and the GPC (chloroform) trace of the filtered solution showed a significantly lower Mn (28 kDa) than the theoretical target value (46 kDa). Supramolecular aggregation of the (racemic) helices formed from **PA7** might be responsible for the observed difficulty in filtration which might have resulted in a fractionation of the polymer.

^{1}H-NMR end group analysis, on the other hand, gave an Mn=40.4 kDa which was in good agreement with the theoretical target value (Supplementary Fig. 209 and Supplementary Table 1). It is worth noting that even assuming the lower Mn (28kDa), polymer **PA7** is the highest molar mass polyaramide prepared by a living polymerization technique to date. This might be due to the fact that a bi-functional initiator was used which introduced a structural disruption from aggregation at the center of the polymer chain and thus increased the polymer's solubility.

In order to obtain additional proof for the living behavior of the new polymerization method, we prepared a macroinitiator consisting of a polyethylene glycol (PEG) mono methyl ether terminated as an *N*-ethylhexyl aminobenzoate (**I6**, Mn=2700 g mol^{-1}, Đ=1.08). Using monomer **A** in an **I6** initiated polymerization using **PHOS1** gave a monodisperse block copolymer (**PA8**, Mn=6600 g mol^{-1}, Đ=1.08) with a shifted SEC trace compared to the macroinitiator **I6** (Fig. 3a and Supplementary Fig. 31).

A statistical copolymer consisting of *N*-ethylhexyl-norbornene-5,6-dicarboximide and *N*-(4-aminophenyl)-norbornene-5,6-dicarboximide was prepared by ring opening metathesis polymerization using Grubbs' 3rd generation initiator. This copolymer served as a macroinitiator (**I7**, Mn=4300, Đ=1.2) for a "grafting-from" copolymerization using monomer **A** and **PHOS1**. The polymer obtained (**PA9**, Mn=25600, Đ=1.18) showed a monomodal SEC trace shifted from the SEC trace of the original macroinitiator **I7** (Fig. 3g and Supplementary Fig. 32). Both macroinitiated polymerizations support a living chain growth polymerization behavior for monomer **A** under **PHOS1** activation conditions.

A monomer (**K**) structurally similar to **A** but *(R)-N*-chirally substituted (Fig. 1 K) was polymerized using initiator **I5** and **PHOS1**. Two chiral polymers were obtained (**PK1**: Mn=3.6 kDa, Đ =1.1; **PK2**: Mn=6 kDa, Đ =1.09) which were investigated by circular dichroism spectroscopy in chloroform at 5°C. In a previous report of this polymer the monomer carried an (*S)*-configured chiral center in the side chain. Here, we used the enantiomeric form of the previously reported monomer and a mirror image of the reported CD-spectrum was observed for its polymer (Supplementary Fig. 301, 303).[36]

In order to show the functional group tolerance of our new method, we prepared monomer **N** carrying an ester and a primary alkyl bromide functionality. Two polymers were prepared from **N** initiated with **I1** using the **PHOS1** reagent (**PN1**: Mn=2.3 kDa, Đ =1.08; **PN2**: Mn=4.2 kDa, Đ =1.07) both showing narrow dispersity. Even though these polymers were merely synthesized as a proof of principle, they could be envisaged to serve as ATRP macro initiators to prepare graft copolymers for example.

To investigate if larger aromatic amino acids could also be polymerized under self-deactivation conditions, we then investigated monomer 6-((2-ethylhexyl)amino)-2-naphthoic acid (monomer **C**, Fig. 1), which had already been polymerized successfully by Yokozawa et al.[37] The polymerization was initiated with **I5** and the carboxylic acid activated using **PHOS1**. A linear relationship between varying [**C**]:[**I5**] ratios and number average molar mass (SEC, $CHCl_3$) showed the living character of the polymerization (**PC1**-**PC3**, Fig. 2b). Additionally, (S)-6-((2-citronellyl)amino)-2-naphthoic acid (**D**) was polymerized using **PHOS1** and initiator

I5 to give polymer **PD1** (Mn=6400 g mol^{-1}, Đ =1.2). The higher dispersities compared to the *p*-aminobenzoic acid derivatives (**A**) investigated before are attributed to the reduced solubility of the formed polymers (**PC1**-**PC3** and **PD1**, Supplementary Table 3) in the polymerization solvent (DCM) as was previously reported.[38,39] It was previously shown that **PD1** can form helical polymers in solutions.[37] Circular dichroism spectroscopy of **PD1** in cyclohexane at 5°C confirmed the reported negative Cotton effect (Supplementary Fig. 299).[37]

Meta substituted aminobenzoic acids had also previously been polymerized under living chain growth conditions.[40,41] Under reversed polarity conditions reported here, we polymerized monomer 3-((2-ethylhexyl)amino)-benzoic acid (monomer **E**, Fig. 1) initiated with **I5** and activated with **PHOS1**. The polymer obtained (**PE1**) showed poor molecular weight control and a broad dispersity (Đ=1.6, Supplementary Table 4) indicating that self-initiation might have occurred to some degree. Cooling the polymerization to -40°C resulted in better dispersities if low molar masses were aimed for (**PE2**, Mn=2400 g mol^{-1}, Đ=1.1) but broader dispersities for higher molar mass polymers (**PE3**, Mn=5200 g mol^{-1}, Đ=1.25). This indicated that self-deactivation of *m*-aminobenzoyl chloride derivatives under reversed polarity conditions was less effective than in the case of Yokozawa et al.[40,41]. Basic ab-initio calculations (DFT, ωB97X-D/ 6-311+G(2DF,2P)) of the frontier orbital energy levels of the deactivated monomers confirmed the observed differences between meta-substituted monomers in Yokozawa's case and ours (Supplementary Fig. 323).

Nonetheless, given that the **PHOS1** activation of aromatic carboxylic acids is extremely fast and tolerant towards secondary aromatic amines, we hypothesized that a pseudo-living polycondensation of monomer **E** could still be achieved if the monomer was added slowly to a solution of activator (**PHOS1**) and initiator (**I5**).

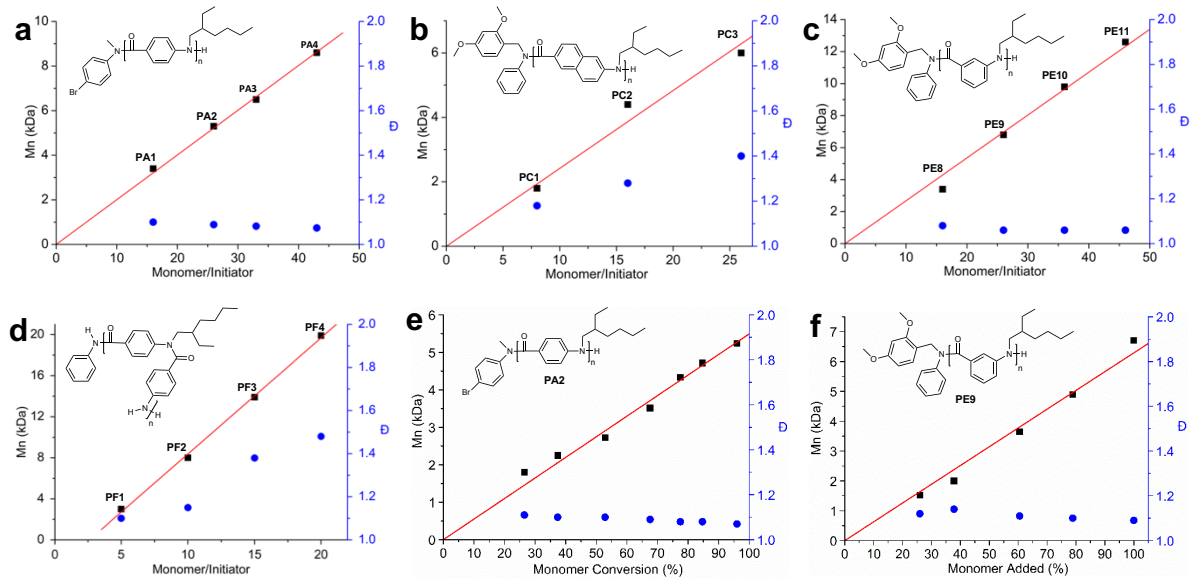

Fig. 2 SEC analysis showing the living nature of the polymers prepared. **a**,**b**,**c**,**d**, Number average molar mass (M_n, SEC) is plotted (black squares) vs. the monomer:initiator ratio. **a**, monomer **A**, initiator **I1**, **PHOS1** activation, **b**, monomer **C**, initiator **I5**, **PHOS1** activation, **c,** monomer **E**, initiator **I5**, **PHOS1** activation, **d,** monomer **F**, initiator **I8**, **PHOS2** activation. **e**, monomer **A**, initiator **I1**, **PHOS1** activation, **f**, monomer **E**, initiator **I5**, **PHOS1**. **e**,**f**, Number average molar mass (M_n, SEC) is plotted vs. monomer conversion (calculated from ^{1}H-NMR spectra). Dispersity values (Đ=M_w/M_n) of the polymer samples are plotted as blue circles. Linear fits are shown as red lines. All data points were obtained by single measurements.

c d

Ideally, the slow monomer addition would result in low concentrations of the activated monomer, thereby dramatically lowering the rate of any bimolecular step-growth condensation reactions.
The reaction of the activated monomer with the initiator, present at a much higher concentration than the monomer, on the other hand, should occur more rapidly. Slow monomer addition to obtain quasi-living conditions have been reported previously as a means to suppress bimolecular side reactions of the monomer.[42,43,44]
In our case, a DCM solution of **E** was added slowly via a syringe pump to a solution of **I5** and **PHOS1** in DCM. The obtained polymers (**PE4**-**PE12**) showed excellent molar mass control as aimed for via the [**E**]:[**I5**] ratio (Supplementary Table 4). It could furthermore be shown that the dispersities were directly related to the speed of monomer addition. Fast addition (0.6 mL h^{-1}) resulted in broader dispersity polymers (**PE4**-**PE7, PE12**, Đ=1.14-1.26) whereas slower addition (0.2 mL h^{-1}) gave excellent dispersities (**PE8**-**PE11**, Đ=1.06-1.08, Supplementary Table 4). We believe that this is an important improvement over previously available methods as even such monomers can be polymerized in a living fashion that lack the structural and electronic requirements for self-deactivation. As shown in Fig. 2c, the molar mass of polymers **PE8-11** increased linearly with the [**E**]:[**I5**] ratio. For the polymerization to form **PE9**, samples were taken from the reaction mixtures at different reaction times. The molar mass of the polymer formed was analyzed by GPC(THF) and the monomer conversion determined by the amount of monomer added via the syringe pump. Fig. 2f shows the linear relationship between molar mass and the monomer conversion as expected for a living polymerization (Supplementary Fig. 40 and Supplementary Table 5). Furthermore, we could also show that monomer **E**, initiated with **I1** could be activated with **PHOS1** and polymerized in a living manner in both acetonitrile (**PE14**, Mn=3.2 kDa, Đ=1.1, Supplementary Fig. 151) and THF (**PE13**, Mn=3 kDa, Đ=1.12, Supplementary Fig. 150). This further emphasized the versatility of the phosphine activation in different solvents.

Scope of the PHOS2 reagent
Encouraged by this observation, we wanted to investigate the polymerization of aromatic amino acids carrying primary amines. As the reagent **PHOS1** could not be employed, we investigated the ICl adduct of tris(*o*-methoxyphenyl)phosphine ((*o*-MeOPh)$_3$P/ICl), **PHOS2** (Supplementary Fig. 13-15). We believed that a lowered electrophilicity and increased steric hindrance of this reagent could render it inert towards primary aromatic amines. **PHOS2** requires the addition of pyridine to activate carboxylic acids and its reaction with aliphatic alcohols yields predominantly the elimination product (Supplementary Scheme 1 and Supplementary Fig. 4, 27). These observations support an increased steric demand of the reagent and a lower electrophilicity of the phosphorous center. The x-ray crystal structure of **PHOS2** exclusively shows the chlorophosphonium iodide (Fig. 1). One of the methoxy groups is positioned towards the phosphorous atom on the opposite side of the P-Cl bond (Fig. 1 and Supplementary Fig. 105). Assuming this is the predominant conformation in non-polar solvents such as DCM this could explain the observed higher selectivity of **PHOS2**. We speculate that aromatic substitution in triarylphosphine reagents might allow the synthesis of even more selective carboxylic acid activation reagents in the future. Furthermore, following a reaction between **PHOS2** and aniline by ^{31}P-NMR spectroscopy showed no reaction over time (1h, Supplementary Fig. 15).

Polymerizations of non-self-deactivating monomers carrying primary amines
The polymerization of aromatic amino acids carrying primary amines is often hindered by the formation of strong hydrogen bonds from secondary amides formed in these polymers.

Furthermore, aromatic amino acids carrying primary amines cannot be polymerized using Yokozawa's method as the resulting acidic secondary amides would immediately be deprotonated. For this reason, no living polymerizations of such amino acids have been reported to date.

Our polymerization method can overcome this limitation and is, furthermore, not limited to self-deactivating monomer structures. Therefore, we chose a dimeric amino acid monomer, 4-(4-amino-*N*-(2-ethylhexyl)benzamido)benzoic acid (**F**). We anticipated that the tertiary amide in **F** would adopt an *E*-configuration (*cis* with respect to the two phenyl rings) which, together with the *N*-alkyl group, would help in increasing the solubility of the polymer. The amine and carboxylic acid functionalities are far removed from each other in **F** such that no self-deactivation for the activated form of **F** could be envisaged.

A first polymerization attempt whereby a solution of **F** was added slowly via a syringe pump to a mixture of **PHOS2**, pyridine and aniline (**I8**) in DCM, gave a polymer (**PF1**, Mn=3000 g mol^{-1}, Đ=1.1) with narrow dispersity. When targeting higher molar mass polymers an almost perfect linear relationship between the [monomer]:[initiator] ratio was observed (Fig. 2d). Unfortunately, the dispersities of the polymers (**PF2**-**PF4**, Supplementary Table 6) also increased. We believe that this is due to aggregation of the polymers via hydrogen bonds in the polymerization solvent (DCM) as the polymers **PF3** and **PF4** were also insoluble in chloroform after precipitation in methanol.

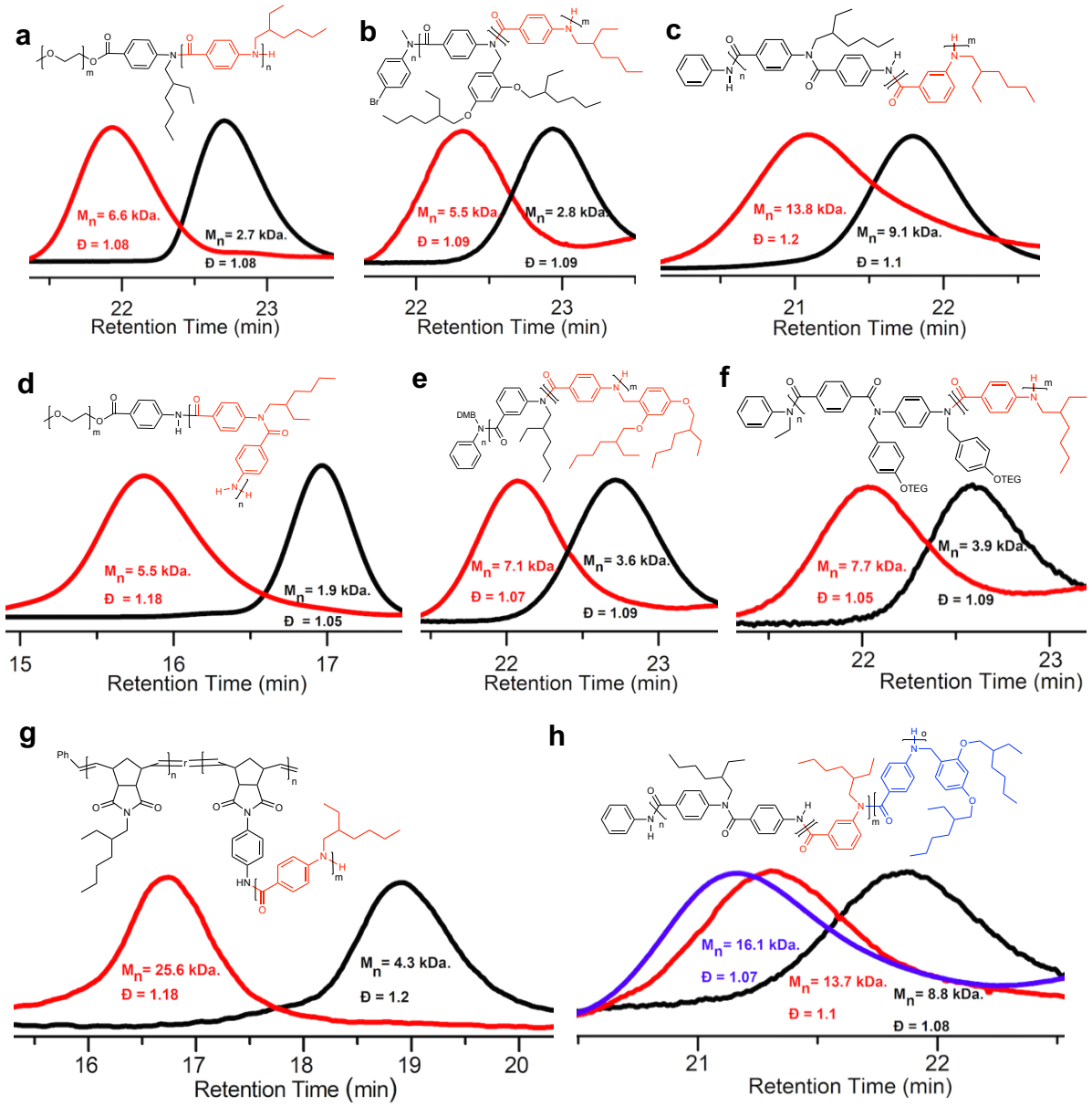

Fig. 3 SEC analysis of copolymers. The structure and SEC curve of the first polymer block or macroinitiator is shown in black, the second block in red and the third block in blue. **a**, **PA8**, monomer **A** initiated with macroinitiator **I6 b**, **PBA1 c**, **PFE1 d**, **PF5**, monomer **F** initiated with macroinitiator **I9 e**, **PEB1 f**, **PMA1 g**, **PA9**, monomer **A** initiated with macroinitiator **I7**, r denotes the random copolymerization of the two metathesis monomers of the main polymer chain **h**, **PFEB1.**

We then carried out another polymerization where **F** was slowly added to a 4-aminobenzoate terminated PEG monomethyl ether macro initiator (**I9,** Mn=1900 g mol^{-1}, Đ=1.05) using **PHOS2**. The polymer obtained (**PF5**, Mn=5500 g mol^{-1}, Đ=1.05) showed very good solubility in both, DMF and chloroform and a very narrow dispersity (Fig. 3d and Supplementary Table 7, Supplementary Fig. 43, 44). This suggests that aggregation of **PF2-PF4** was most likely the reason for the observed higher dispersities (see above).
A dimeric monomer (**L**) which is structurally similar to **F** but carrying a chiral side chain on the amide nitrogen atom (Fig. 1 L) was polymerized using initiator **I8** and **PHOS2** (**PL1**: Mn=2.9 kDa, Đ=1.17; **PL2**: Mn=12.4 kDa, Đ=1.23). Two narrow dispersity polymers (**PL1** and **PL2**) could be prepared. Chloroform solutions were used to measure circular dichroism

spectra which resembled those of well-defined oligomers of **L** reported previously (Supplementary Fig. 305, 307).[45]
Finally, the dimeric monomer **M** was synthesized and polymerized. Monomer **M** represents the *N*-protected AABB repeat unit of the commercial polymer Kevlar®. Polymer **PM1** was obtained when the monomer was slowly added to a mixture of initiator **I1** and **PHOS1** (Mn=3.9 kDa, Đ=1.1).

Block copolymerizations
One critically important feature of any living polymerizations is its capability to form block copolymers. All block copolymerizations regardless of the monomer employed were carried out using the slow monomer addition method. This allowed a convenient sequential addition of monomers by syringe pump without the need to follow monomer consumption over the course of the polymerization. Each polymer block was analyzed by ^{1}H-NMR spectroscopy to confirm full monomer conversion after complete monomer addition. Additionally, GPC analysis was carried out after each block formation.
First, a diblock copolymer was prepared using initiator **I1**, **PHOS1** and slow addition of monomers **B** and **A** sequentially (first block: Mn=2.8 kDa, Đ =1.09, diblock: Mn=5.5 kDa, Đ=1.09, Fig. 3b and Supplementary Fig. 33). GPC(THF) analysis confirmed a clear shift of the molar mass distribution from the first block to the diblock copolymer (**PBA1**), as expected for a living polymerization (Fig. 3b). Next, we polymerized monomers **F** and **E** sequentially using **PHOS2** as monomer **F** carried a primary amine. The polymerization was initiated with aniline (**I8**). As before, GPC(THF) analysis showed a distinct shift from the first polymer block (Mn=9.1 kDa, Đ=1.1) to the diblock copolymer (**PFE1**, Mn=13.8 kDa, Đ=1.2, Fig. 3c and Supplementary Fig. 46). We then prepared a diblock copolymer in which the first block was synthesized from an *N*-alkyl *m*-aminobenzoic acid, followed by a second block consisting of an *N*-alkyl *p*-aminobenzoic acid monomer (Fig. 3e and Supplementary Fig. 41, **PEB1**, first block: Mn=3.6kDa Đ=1.09, diblock: Mn=7.1 kDa, Đ=1.07, activation via **PHOS1**). To further show the potential of our method, we next prepared a diblock copolymer from monomer **M**, followed by monomer **A**, initiated by **I10** (Fig. 3f and Supplementary Fig. 50, **PMA1**). Sequential copolymerization of both blocks showed the living character of the polymerization of each block (first block: Mn=3.9 kDa, Đ=1.09, diblock: Mn= 7.7 kDa, Đ=1.05, activation via **PHOS1**). The monomer **M** was *N*-protected in order to prevent solution aggregation during polymerization as Kevlar® is well-known for its strong hydrogen bond formation capabilities. To the best of our knowledge, this is the first report of a living Kevlar® polymerization. Finally, we synthesized a triblock terpolymer via sequential addition of monomers **F**, **E** and **B**, initiated by aniline (**I8**) and activated via **PHOS2** (Fig. 3h and Supplementary Fig. 47, **PFEB1**). Narrow dispersities could be observed after addition of each polymer block (first block: Mn=8.8 kDa, Đ=1.08, diblock: Mn=13.7 kDa, Đ=1.1, triblock: Mn=16.1 kDa, Đ=1.07). Incorporation of well-defined aggregating polyaramids into block copolymer architectures could be important for supramolecular solution aggregation and bulk materials applications in the future.
These results clearly show that the **PHOS2** activation system is capable of activating aromatic carboxylic acids in the presence of primary aromatic amines (monomers **F**, **G** and **L**) and that both phosphonium activators (**PHOS1** and **PHOS2**) can be used under slow monomer addition conditions. Furthermore, the ability to polymerize aromatic amino acid oligomers opens up the possibility to synthesize well-defined polymers with monomer sequence control.

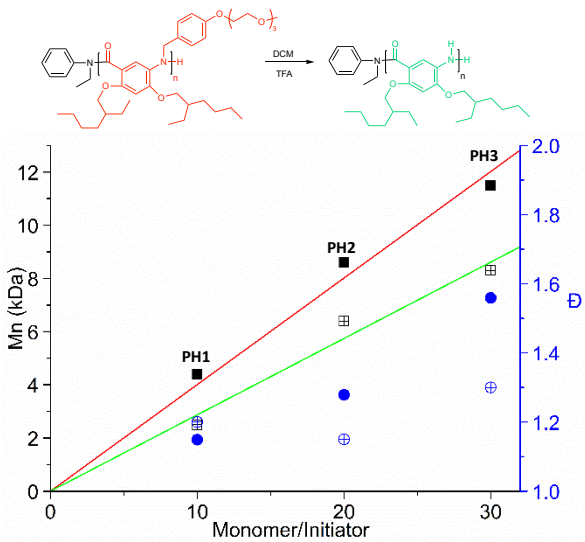

Fig. 4 SEC analysis of polymers **PH1**-**PH3** before and after *N*-deprotection. After *N*-deprotection, the polymer folds into a helical structure. Solid squares: M_n values before *N*-deprotection, solid blue circles: dispersity values before *N*-deprotection. Open squares: M_n values after *N*-deprotection, i.e. helix formation, open circles: dispersity values after *N*-deprotection, i.e. helix formation. Straight lines represent linear fits of the M_n values. Dispersity values ($Đ=M_w/M_n$) of the polymer samples are plotted as blue circles. Squares refer to the (left, black) molecular weight axis, circles to the (right, blue) dispersity axis. All data points were obtained by single measurements.

Polymerization of helical foldamers

Helical aramide foldamers are an important class of oligoaramids that are currently under investigation as potential biological membrane transport channels, due to their tubular folded architectures. However, the highly functional monomers from which these tubular structures are prepared have so far never been polymerized in a living fashion. Therefore, we synthesized 5-amino-2,4-bis((2-ethylhexyl)oxy)benzoic acid (monomer **G**) and polymerized it via slow addition (0.06 mL/h) to a mixture of initiator **I8** and **PHOS2** to give polymer **PG1** (Mn=7000 g mol^{-1}, Đ=1.2). Oligomers of derivatives of **G** have previously been shown to fold into helical foldamers by Gong et al.[24] All attempts to obtain higher molar masses by varying the [**G**]:[**I8**] ratio failed and yielded polymers with similar number average molar masses as **PG1**. We attribute this to an increased steric demand of the chain end of the helical polymers and, possibly, the formation of supramolecular aggregates in DCM solution which prevent access to the reactive amine chain end.[46]

To circumvent this limitation, we *N*-protected monomer **G** with the acid labile 4-(2-(2-(2-methoxyethoxy)ethoxy)ethoxy)-benzyl group to give monomer **H**. Polymerization of **H** by slow addition of **H** to a mixture of initiator *N*-ethylaniline (**I10**) and **PHOS2** allowed us to synthesize *N*-protected polymers **PH1**-**PH3** (**PH1**: monomer addition rate=0.1mL/h, Mn=4400 g mol^{-1}, Đ=1.15, **PH2**: rate=0.08 mL/h, Mn=8600 g mol^{-1}, Đ=1.28, **PH3**: rate=0.08 mL/h, Mn=11500 g mol^{-1}, Đ=1.56) with good molar mass control (Fig. 4 and Supplementary Table 8).

As these polymers represent *N*-protected tertiary amides, we *N*-de-protected them using a mixture of DCM, trifluoroacetic acid and triisopropylsilane (50:49:1, Supplementary Fig. 49). The resulting polymers were, once again, analyzed using SEC, showing remarkably different molar masses and dispersities to before (after cleavage of the *N*-protecting group, **PH1C**: Mn=2500 g mol^{-1}, Đ=1.21, **PH2C**: Mn=6400 g mol^{-1}, Đ=1.15, **PH3C**: Mn=8300 g mol^{-1}, Đ=1.32, Supplementary Table 8). Polymers **PH1**-**PH3** and **PH1C**-**PH3C** showed good

solubility in the SEC solvent DMF. Furthermore, the additive LiBr (0.1%) most likely suppressed any intramolecular hydrogen bonding, i.e. helix formation for **PH1C-PH3C**. Nonetheless, the tertiary aromatic amides in **PH1-PH3** will adopt a *cis* configuration (with respect to the two phenyl rings) while the secondary amides in **PH1C-PH3C** will adopt a *trans* configuration (with respect to the phenyl rings).[47] **PH1C-PH3C** will, therefore, be conformationally more restricted and adopt a more rigid solution structure even in the absence of helix formation. We hypothesize that the decrease in dispersity is a direct result of the change of the shape of the macromolecule in solution.

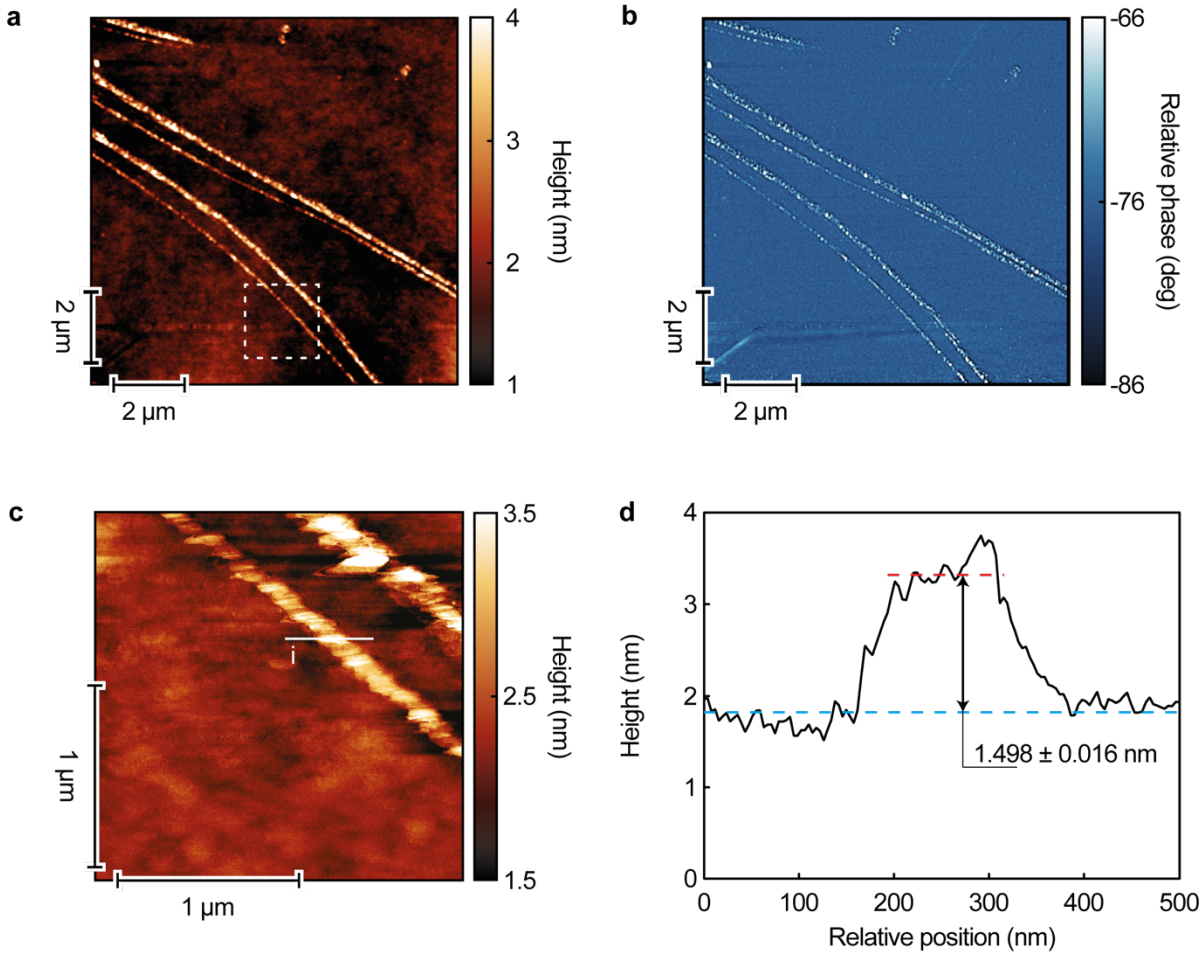

Fig. 5 AFM analysis of helical polymer **PJ1C** with a declared tip radius of less than 10nm. **a**, Height data of region with low magnification, box highlight corresponds to high magnification data in **c**. **b**, Phase data of region shown in **a**. **c**, Height data of region highlighted in **a** showing the helicoidal structure of the molecular assembly. **d**, profile (i) of selection highlighted in **c**, measured diameter of the helix is of 1.498 ± 0.016 nm (please consider that lateral dimension contains systematic error, for further details please refer to the Supporting text Instrumentation section).

Having established the excellent molecular weight control during the polymerization of **H**, we next used **PHOS2** to polymerize a derivative of **H**, monomer **J** (Fig. 1) carrying a more polar triethylene glycol derived side chain (**PJ1**: Mn=8300 g mol^{-1}, Đ=1.18). After cleavage of the *N*-protective groups, a polymer was obtained (**PJ1C**: Mn=4000 g mol^{-1}, Đ=1.13) which was both, chloroform and water soluble. In analogy to Gong's observation, **PJ1C** was assumed to adopt a helical conformation in solution.[24] To confirm, we prepared aqueous **PJ1C** solutions which were drop-cast onto glass slides and investigated by atomic force microscopy (AFM,

Fig. 5 and Supplementary Fig. 297, 298). The AFM images (Fig. 5 a, b, d) show straight linear structures with a height of about 1.5 nm and several micrometers in length. We believe that these structures are end-to-end aggregates of individual short helical polymer chains. The fine structure observed along these aggregates furthermore supports the presence of a helix (Fig. 5 c). We believe that the well-defined polymeric foldamers shown in the AFM images above illustrate the potential that the new polymerization method described here can play in the growing field of aromatic amide foldamers. Due to its fast acid activation and high aromatic amine tolerance it is conceivable that slow monomer addition will allow many aromatic amino acids to be polymerized in a living fashion.

In conclusion, we have shown that exchanging the counter ion of the well-known chlorotriphenyl phosphonium cation from chloride to the less nucleophilic iodide (in DCM) results in a milder activation reagent for carboxylic acids. This reagent can be synthesized from Ph_3P and the interhalogen reagent ICl. It activates aromatic carboxylic acids as acid chlorides in the presence of aromatic secondary amines. *Para*-substituted amino acid chlorides, that can be prepared using this reagent, are electronically self-deactivated and cannot self-initiate polymerization. In the presence of amine initiators, living polyamides can be obtained. Due to the fast acid activation, even non self-deactivating monomers such as *meta*-amino acids can be polymerized in a living fashion by slow addition, thereby avoiding step growth side reactions. Tri(*o*-methoxyphenyl)phosphine activated with ICl gives a sterically more demanding reagent that activates aromatic carboxylic acids as acid chlorides in the presence of primary aromatic amines. This allows the synthesis of polyaramides containing secondary amides. Using these two reagents we could show the living polymerization of para and meta-substituted primary and secondary amino benzoic acids. Narrow dispersity homopolymers, diblock copolymers and also a triblock terpolymer were prepared. Furthermore, aromatic amino acid oligomers could also be polymerized in a living fashion as shown in the formation of a diblock copolymer in which one of the two blocks consisted of an *N*-protected living Kevlar® block.

Helical aramid foldamers are known to forming channel-like structures capable of transporting small molecules. Here we show that typical monomers from which such helical foldamers are prepared can be polymerized in a living fashion using slow monomer addition. An example of such a helical polymer was prepared and investigated by AFM microscopy. The images obtained are in excellent agreement with the assumed helical structure. This illustrates the huge potential of this new polymerization method for the field of polymeric aromatic foldamers and well-defined supramolecular polymers based on aromatic amides (aramides) and their copolymers in general.

Data availability

All data generated and analysed during this study are included in this Article and its Supplementary Information. Crystallographic data for the structures reported in this Article have been deposited at the Cambridge Crystallographic Data Centre, under deposition numbers CCDC 1983404 (**PHOS1**) and 1983405 (**PHOS2)**. Copies of the data can be obtained free of charge via www.ccdc.cam.ac.uk/data_request/cif.

Acknowledgements

We thank A. Coskun and S. Salentinig for helpful comments and F. Karasu Kilic for GPC measurements. Funding was provided by the National Center for Competence in Research (NCCR) "Bio-Inspired Materials".

Author contributions: S.P. and A.F.M.K. designed the experiments, S.P. synthesized all phosphorous reagents, performed all polymerizations and carried out all molecular and

polymer analysis. D.P.T.N. and M.A. synthesized monomers, A.M. repeated and confirmed the polymerization experiments. A.C. performed the x-ray single crystal analysis, R.O. and A.F. performed atomic force microscope measurements. All authors reviewed the manuscript.

Competing interests
The authors declare no competing interests.

Additional Information
Supplementary information
Materials and Instrumentation. Syntheses of monomers, initiators, activation reagents and polymers. NMR, GPC, MALDI-ToF MS, high resolution mass spectra, AFM analyses, UV absorption and fluorescence spectra, circular dichroism spectra and ab-initio calculations.

Crystallographic Data
Crystallographic data for compound **PHOS1**. CCDC reference 1983404.

Crystallographic data for compound **PHOS2**. CCDC reference 1983405.

Methods
Here, the synthesis of the two activating phosphine reagents **PHOS1** and **PHOS2** is described as well as two examples for polymerizations: one under "one-pot" self-deactivation conditions and the other via slow monomer addition. A complete description of all experimental methods is found in the Supplementary Information Section.

Materials
Anhydrous triphenylphosphine (*ReagentPlus*®, 99%), 1M iodine monochloride solution in dichloromethane, iodine, 3-bromo-*N*-methylaniline (**I1**), 4-aminobenzoic acid, 4-nitrobenzoyl chloride, Pd on carbon (10 wt. % loading) and 2-ethylhexanal (96%) were purchased from Acros Organics and used without further purification. Anhydrous pyridine, triphenylphosphine oxide, methyl 4-aminobenzoate (**I2**), aniline (**I8**), *N*-ethylaniline (**I10**), 2,4-dimethoxybenzaldehyde, 3-aminobenzoic acid and methoxy poly(ethylene glycol) were purchased from Sigma Aldrich and used without further purification. Sodium triacetoxyborohydride and 6-amino-2-naphthoic acid were purchased from Fluorochem. All other reagents and solvents were purchased from Acros Organics or Sigma-Aldrich and used without further purification. Phenyl 4-((2,4-dimethoxybenzyl)amino)benzoate (**I3**), phenyl 4-((2-ethylhexyl)amino)benzoate, 2, 4-bis((2-ethylhexyl)oxy)benzaldehyde, exo-*N* - ethylhexylnorbornene imide were synthesized as reported previously.[48,49,50] Deuterated solvents (CD_2Cl_2, $CDCl_3$ and DMSO-d_6) were purchased from Cambridge Isotope Laboratories, Inc. All polymerization reactions were performed in flame-dried glassware under inert atmosphere utilizing standard Schlenk line techniques.

Instrumentation
All ^1H NMR, ^{13}C NMR and ^{31}P NMR spectra were recorded on a Bruker Avance DPX (400 MHz and 300 MHz) FT NMR spectrometer. Chemical shifts for ^1H and ^{13}C were given in ppm relative to the residual solvent peak ($CDCl_3$: 7.26 for ^1H; $CDCl_3$: 77.16 for ^{13}C and CD_2Cl_2: 5.32 for ^1H; CD_2Cl_2: 53.84 for ^{13}C) and ^{31}P was given in ppm relative to internal reference (85% phosphoric acid sealed inside capillaries). HR MALDI FT-ICR mass spectra were measured on a Bruker FTMS 4.7T BioAPEX II in positive mode using trans-2-[3-(tert-butylphenyl)-2-methyl-2-propenylidene] malononitrile (DCTB) as matrix and sodium trifluoroacetate (NaTFA) as the counter ion source. HR-MS (ESI+) mass spectra were

measured on a Bruker FTMS 4.7T BioAPEX II and Thermo Scientific LTQ Orbitrap XL equipped with a static nanospray ion source. Electron impact ionization mass spectra (EI-MS) were run on a gas chromatography - mass spectrometry (GC-MS) instrument (Thermo Scientific DSQ II Series Single GC/MS with Trace GC Ultra gas chromatograph and Zebron capillary GC column (ZB-5MS, 0.25 μm, 30 x 0.25 mm). Relative molecular weights and molecular weight distributions were measured by gel permeation chromatography (GPC) with either tetrahydrofuran, chloroform or DMF as eluent with a flow rate of 1 mL/min at 40°C, 40°C and 60°C respectively. The THF and chloroform GPC systems were calibrated with polystyrene standards in a range from 10^3 to 3×10^6 Da. The THF GPC is an automated Viscotek GPCmax VE-2001 with a set of two Viscotek T6000M linear columns (300 x 8 mm, 5 μm particle size). Signal detection occurred by use of a Viscotek VE 3580 RI detector (refractive index). The Chloroform GPC is an automated PSS SECcurity System (Agilent Technologies 1260 infinity ll) with a set of two MZ-Gel SDplus linear columns (300 x 8 mm, 5 μm particle size). The DMF GPC is an automated Agilent 1260 Infinity II HPLC system equipped with one Agilent PolarGel M guard column (particle size = 8 μm) and two Agilent PolarGel M columns (ID = 7.5 mm, L = 300 mm, particle size = 8 μm). Signals were recorded by a UV detector (Agilent 1260 series) and an interferometric refractometer (Agilent 1260 series). Samples were run using DMF + 0.05M LiBr as the eluent at 60 °C and a flow rate of 1.0 mL/min. Molecular weights were determined based on narrow molecular weight poly(ethylene oxide) calibration standards.
All polymer samples were filtered through a PTFE syringe membrane filter (0.45 μm pore size, VWR) prior to GPC measurements. The polymers were purified by JAI LCI9130 recycling GPC with $CHCl_3$ as the eluent. The system consisted of two linear JaigelI2H and JaigelI1H columns. Signal detection was performed with a UV 600 Next detector. Slow additions of the monomers into the reaction mixtures were conducted using a syringe pump (World Precision Instruments, SP100iZ) equipped with a BD syringe and a needle measuring 0.8 mm in diameter.
Single crystals of **PHOS1** and **PHOS2** were obtained by recrystallisation from DCM solution by slow evaporation. Suitable crystals were selected and mounted on a loop in oil on a Stoe IPDS2 diffractometer. The crystal was kept at 250(2) K during data collection. Using Olex2, the structure was solved with the ShelXT structure solution program using Intrinsic Phasing and refined with the ShelXL refinement package using Least Squares minimization.[51,52,53] Hydrogen positions on carbons were refined with riding coordinates with a fixed Uiso (1.2 times). In case of compound **PHOS1**, 42 restraints have been used with carbon atoms from phenyl rings (C7 -> C12) defined with a similar Uiso; site of occupation factors (s.o.f.) of the iodine and chlorine atoms were refined as dependent group (s.o.f. of Cl1A, I1A 0.780(3) and s.o.f. of Cl1B, I1B 0.220(3)). The Diamond program was used to prepare drawings.[54]
CCDC 1983404 and CCDC 1983405 contain the supplementary crystallographic data for **PHOS1** and **PHOS2**, respectively. These data can be obtained free of charge via http://www.ccdc.cam.ac.uk/conts/retrieving.html, or from the Cambridge Crystallographic Data Centre, 12 Union Road, Cambridge CB2 1EZ, UK; fax: (+44) 1223-336-033; or e-mail: deposit@ccdc.cam.ac.uk.

AFM images were taken with the use of a Park NX10 instrument (Park Systems Corp., Suwon, Korea), equipped with Smart Scan software version 1.0 RTM 12d. All measurements were performed in an acoustic enclosure (JPK Instruments AG, Berlin, Germany) equipped with antivibration table (e-Stable mini, Kurashicki Kako Co., LTD, Okayama, Japan). Tips used for imaging were TAP300AL-G (Budget Sensors, Sofia, Bulgaria) with declared tip radius of less than 10 nm and NSG30_SS (NT-MDT Spectrum instruments, Moscow, Russia) with declared tip radius of less than 5 nm. No tip deconvolution was applied to images inducing a systematic

error in the XY plane size definition and highly dependent on the exact tip shape and size.[55] Tips spring constants and instrument sensitivity were measured after each tip was mounted with the use of the Sader method[56] and with tip displacement method[57] respectively. For all tips tip spring constants were within the declared range declared by manufacturers. All images were taken in tapping mode, with oscillation set point of 20 ± 10 nm, integral gain of 0.1 ± 0.2 A.U., proportional gain of 0.1 ± 2 A.U., scanning rate of 0.7 ± 0.3 Hz and with imaging size of 512x512 pixels. Raw data was elaborated with the use of Gwyddion software (Version 2.54, GNU licencing). All data was treated in the same way. AFM data was levelled by "mean plane subtraction", followed by "polynomial baseline removal" of second order in both fast and slow scan directions. Look up table (LUT) was adjusted to increase contrast of image features. Fitting of profiles was done with the use of MATLAB software (MathWorks, Natick), with a second order polynomial fitting through a minimization of the least square residuals of the individual lobes of the profile.
UV-Vis absorption spectra were measured on a Jasco V-630 spectrophotometer. Fluorescence spectra were performed on a Jasco FP-6200 spectrofluorometer. All spectroscopic measurements were performed either in spectroscopic grade $CHCl_3$ or cyclohexane.
Circular dichroism spectra were recorded on a Jobin Yvon Auto Dichrograph Mark V which was temperature controlled via a ThermoMetric 5510 Thermostat. Data was recorded using a personal computer running Ubuntu 18.04 with a custom made recording software (python) and a custom made hardware interface (Arduino Uno).
Ab-initio calculations were carried out using Spartan 18 v 1.4.4 (Wavefunction Inc.).

*Synthesis of triphenylphosphine iodochloride (**PHOS1**)*
A Schlenk flask containing triphenylphosphine (20 g, 76.3 mmol, 1.08eq) was evacuated and backfilled with argon three times. The triphenylphosphine was dissolved in dry DCM (50 mL) and was cooled to 0°C. To this solution iodine monochloride (70.6 mL, 1M solution in DCM, 70.6 mmol, 1eq) was added dropwise. The reaction mixture was allowed to warm to RT and stirred for further 30 min. The solvent was evaporated under exclusion of air and moisture to obtain a yellow solid (29.6 g, 99%) which was washed with dry pentane (100mL) under an argon atmosphere. The solid was stored in an argon filled glove box and used without further purification. ^{1}H NMR (400 MHz, DICHLOROMETHANE-d_2) δ 7.20 - 8.37 (m, 15 H) ppm. ^{31}P NMR (162 MHz, DICHLOROMETHANE-d_2) δ 65.8, 32.3, -16.7 ppm. ^{13}C NMR (75 MHz, DICHLOROMETHANE-d_2) δ 137.5 (s), 133.98 (d, J=12.1 Hz), 131.07 (d, J=12.1 Hz), 118.9 (d, J=93.9 Hz) ppm.

*Synthesis of tris(o-methoxyphenyl)phosphine iodochloride (**PHOS2**)*
A Schlenk flask containing tris(o-methoxyphenyl)phosphine (20 g, 56.7 mmol, 1.08eq) was evacuated and backfilled with argon three times. The tris(*o*-methoxyphenyl)phosphine was dissolved in dry DCM (30 mL) and was cooled to 0°C. To this solution iodine monochloride (52.5 mL, 1M solution in DCM, 52.5 mmol, 1eq) was added dropwise. The reaction mixture was allowed to warm to RT and stirred for further 30 min. The solvent was evaporated under exclusion of air and moisture to obtain a yellow solid (26.7 g, 99%) which was washed with dry pentane (10 mL) under an argon atmosphere. The solid was stored in an argon filled glove box and used without further purification. ^{1}H NMR (400 MHz, DICHLOROMETHANE-d_2) δ 7.79 - 7.98 (m, 3 H), 7.35 - 7.47 (m, 3 H), 7.17 - 7.33 (m, 6 H), 3.68 - 3.76 (m, 9 H) ppm. ^{31}P NMR (162 MHz, DICHLOROMETHANE-d_2) δ 57.9 ppm. ^{13}C NMR (75 MHz, DICHLOROMETHANE-d_2) δ 162.25 (d, J=2.75 Hz), 139.23 (d, J=2.20 Hz), 135.00 (d, J=11.55 Hz), 122.41 (d, J=15.41 Hz), 113.71 (d, J=7.15 Hz), 107.08 (d, 103.5 Hz), 57.04 (s) ppm.

Procedure for one pot polymerization of N-substituted-4-aminobenzoic (A/B/K)

A Schlenk flask containing monomer **A**/**B**/**K** (16-150 eq of initiator **I#**, see Table S1) and initiator (**I#**) were evacuated and backfilled with argon three times. The mixture was dissolved in dry DCM (0.8M) and cooled to 0°C. The phosphine complex (**PHOS1**) was weighted (1.6 eq of **A**/**B**) inside an argon filled glove box and transferred to another Schlenk flask. **PHOS1** was dissolved separately in dry DCM (0.8 M) and cooled to 0°C. The precooled monomer and initiator solution was quickly transferred to the **PHOS1** solution and stirred for 30 min at 0°C. To this reaction mixture anhydrous pyridine (5eq of **A/B**) was added quickly and allowed to warm to RT. The conversion of the reaction was followed by ^{1}H NMR spectroscopy. The reaction was quenched with excess water and extracted three times with DCM. The combined organic layer was dried over $MgSO_4$ and concentrated under reduced pressure to obtain the crude polymer. Finally, the polymers were purified by recycling gel permeation chromatography (chloroform).

Procedure for block copolymerization of 4-(4-amino-N-(2-ethylhexyl)benzamido) benzoic acid (F) and 3-((2-ethylhexyl)amino)benzoic acid (E) (PFE1)

The phosphine active complex **PHOS2** (1.04 g, 2 mmol, 75eq) was weighted into a Schlenk flask and dissolved in dry DCM (0.92M). To this solution, anhydrous solution of initiator (**I8**, 2.5 mg, 0.0246 mmol, 1 eq) and anhydrous pyridine (0.43 mL, 425 mg, 5.37 mmol, 80eq) were added. In another Schlenk flask monomer **F** (99 mg, 0.27 mmol, 10eq) was evacuated, backfilled with argon three times. A solution of monomer **F** in dry DCM (0.15M) and anhydrous pyridine (0.17 mL, 171 mg, 2.1 mmol, 8eq of **F**) was added dropwise to the reaction mixture at RT using a syringe pump (0.2 mL/hour). After complete addition of monomer **F**, a sample was collected for GPC analysis (THF GPC $\mathbf{M_{n\text{-}GPC}}$ = 9.1 kDa.; **Đ** = 1.1). Thereafter, in a Schlenk flask monomer **E** (100 mg, 0.4 mmol, 15eq) was evacuated, backfilled with argon three times. Then a solution of monomer **B** in dry DCM (0.15M) was added dropwise to the reaction mixture at RT using a syringe pump (0.2 mL/hour). The crude polymer (**PFE1)** was analyzed by THF GPC ($\mathbf{M_{n\text{-}GPC}}$ = 13.8 kDa.; **Đ** = 1.2). The reaction was quenched with excess water and extracted three times with DCM. The combined organic layer was dried over $MgSO_4$ and concentrated under reduced pressure to obtain crude polymer. Finally, the polymers were precipitated in cold acetonitrile to obtain polymer **PFE1**.

Data availability

The data that support the plots within this manuscript are provided with this paper.

References

1 Carothers, W. H. Polymers and polyfunctionality. *Trans. Faraday Soc.* **32**, 39–49 (1936).

2 Merrifield, R. B. Solid Phase Peptide Synthesis. I. The Synthesis of a Tetrapeptide. *J. Am. Chem. Soc.* **85**, 2149–2154 (1963).

3 Koenig, H. M., Gorelik, T., Kolb, U. & Kilbinger, A. F. M. Supramolecular PEG–co-Oligo(p-benzamide)s Prepared on a Peptide Synthesizer. *J. Am. Chem. Soc.* **129**, 704–708 (2007).

4 Baptiste, B., Douat-Casassus, C., Laxmi-Reddy, K., Godde, F. & Huc, I. Solid Phase Synthesis of Aromatic Oligoamides: Application to Helical Water-Soluble Foldamers. *J. Org. Chem.* **75**, 7175–7185 (2010).

5 Lutz, J.-F. Defining the Field of Sequence-Controlled Polymers. *Macromol Rapid Comm.* **38**, 1700582 (2017).

6 Lutz, J.-F., Ouchi, M., Liu, D. R. & Sawamoto, M. Sequence-Controlled Polymers. *Science* **341**, 1238149–1238149 (2013).

7 Gutekunst, W. R. & Hawker, C. J. A General Approach to Sequence-Controlled Polymers Using Macrocyclic Ring Opening Metathesis Polymerization. *J. Am. Chem. Soc.* **137**, 8038–8041 (2015).

[8] Huang, Z. et. al. Discrete and Stereospecific Oligomers Prepared by Sequential and Alternating Single Unit Monomer Insertion. *J. Am. Chem. Soc.* **140**, 13392–13406 (2018).

[9] Anastasaki, A. et. al. One-Pot Synthesis of ABCDE Multiblock Copolymers with Hydrophobic, Hydrophilic, and Semi-Fluorinated Segments. *Angew. Chem. Int. Edit.* **56**, 14483–14487 (2017).

[10] Dawson, S. J., Hu, X., Claerhout, S. & Huc, I. *Methods in Enzymology*. **580**, 279–301 (2016).

[11] Yokozawa, T. & Yokoyama, A. Chain-Growth Condensation Polymerization for the Synthesis of Well-Defined Condensation Polymers and π-Conjugated Polymers. *Chem Rev.* **109**, 5595–5619 (2009).

[12] Yokozawa, T. & Ohta, Y. Transformation of Step-Growth Polymerization into Living Chain-Growth Polymerization. *Chem Rev* **116**, 1950–1968 (2016).

[13] Yokozawa, T. & Ohta, Y. Scope of controlled synthesis via chain-growth condensation polymerization: from aromatic polyamides to π-conjugated polymers. *Chem Commun.* 49, 8281–8310 (2013).

[14] Badoux, M. & Kilbinger, A. F. M. Synthesis of High Molecular Weight Poly(p-benzamide)s. *Macromolecules* **50**, 4188–4197 (2017).

[15] Yokozawa, T.; Asai, T.; Sugi, R.; Ishigooka, S.; Hiraoka, S. Chain-Growth Polycondensation for Nonbiological Polyamides of Defined Architecture. *J. Am. Chem. Soc.* **122**, 8313-8314 (2000).

[16] Ziach, K. et. al. Single helically folded aromatic oligoamides that mimic the charge surface of double-stranded B-DNA. *Nat Chem.* **10**, 511–518 (2018).

[17] Rogers, J. M. et. al. Ribosomal synthesis and folding of peptide-helical aromatic foldamer hybrids. *Nat Chem.* **10**, 405–412 (2018).

[18] De, S., Chi, B., Granier, T., Qi, T., Maurizot, V. & Huc, I. Designing cooperatively folded abiotic uni- and multimolecular helix bundles. *Nat Chem.* **10**, 51–57 (2018).

[19] Gan, Q. et. al. Translation of rod-like template sequences into homochiral assemblies of stacked helical oligomers. *Nat Nanotechnol.* **12**, 447–452 (2017).

[20] Chandramouli, N. et. al. Iterative design of a helically folded aromatic oligoamide sequence for the selective encapsulation of fructose. *Nat Chem.* **7**, 334–341 (2015).

[21] Gan, Q. et. al. *Science* **331**, 1172–1175 (2011).

[22] Cao, J. et. al. Preparation and helical folding of aromatic polyamides. *Chem. Commun.* **48**, 11112–11114 (2012).

[23] Yuan, L. et. al. Helical Aromatic Oligoamides: Reliable, Readily Predictable Folding from the Combination of Rigidified Structural Motifs. *J. Am. Chem. Soc.* **126**, 16528–16537 (2004).

[24] Gong, B. et. al. *Creating nanocavities of tunable sizes: Hollow helices. Natl. Acad. Sci. Usa* **99**, 11583–11588 (2002).

[25] Leggio, A. et. al. Formation of amides: one-pot condensation of carboxylic acids and amines mediated by $TiCl_4$. *Chemistry Central Journal* **11**, 87 (2017).

[26] Lundberg, H., Tinnis, F., Selander, N. & Adolfsson, H. Catalytic amide formation from non-activated carboxylic acids and amines. *Chem. Soc. Rev.* **43**, 2714–2742 (2014).

[27] Montalbetti, C. & Falque, V. Amide bond formation and peptide coupling. *Tetrahedron* **61**, 10827–10852 (2005).

[28] Ali, M. F. & Harris, G. S. Chlorine-containing Mixed Halogen Adducts of Triphenylphosphine, Triphenylarsine, and Triphenylstibine *J. Chem. Soc. Dalton* **0**, 1545–1549 (1980)

[29] Montanari, V., Quici, S. & Resnati, G. 1-Iodo-Perfluoroalkanes from Polyfluoroalkoxy Trimethylsilanes and Iodochloro Triphenylphosphorane *Tetrahedron Lett.* ***35***, 1941–1944 (1994)

[30] Nikitin, K., Jennings, E. V., Sulaimi, Al, S., Ortin, Y. & Gilheany, D. G. Dynamic Cross-Exchange in Halophosphonium Species: Direct Observation of Stereochemical Inversion in the Course of an S_N2 Process *Angew Chem Int Edit.* **57**, 1480–1484 (2018).

[31] Quin, Louis & Williams, Antony. Practical Interpretation of P-31 NMR Spectra and Computer-Assisted Structure Verification, Advanced Chemistry Development, Inc. Toronto, Canada (2004).

[32] Godfrey, S. M., McAucliffe, C. A., Pritchard, R. G., Sheffield, J. M. & Thompson, G. M. Structure of R_3PCl_2 compounds in the solid state and in solution: dependency of structure on R. Crystal structures of trigonal bipyramidal $(C_6F_5)_3PCl_2$, $Ph_2(C_6F_5)PCl_2$ and of ionic $Pr^n_3PCl_2$ J. *Chem. Soc. Dalton* **0**, 4823-4828 (1997)

[33] Gonnella, N. C., Busacca, C., Campbell, S., Eriksson, M., Grinberg, N., Bartholomeyzik, T., Ma, S., Norwood, D. L. ^{31}P Solid state NMR study of structure and chemical stability of dichlorotriphenylphosphorane *Magn. Reson. Chem.* **47**, 461-464 (2009)

[34] Voronkov, M. G., Vlasova, N. N. & Vlasov, A. V. Acyl iodides in organic and organoelement chemistry. *Russ. Chem. B+* **62**, 1945–1961 (2013).

[35] Hoffmann, H. & Haase, K. The Synthesis of Acyl Iodides. *Synthesis-Stuttgart* 715–719 (1981).

[36] Tanatani, A. et al. Helical Structures of N-Alkylated Poly(p-benzamide)s. *J. Am. Chem. Soc.* **127**, 8553-8561 (2005).

[37] Mikami, K. & Yokozawa, T. Helical folding of poly(naphthalenecarboxamide) in apolar solvent. *J Polym Sci Pol Chem.* **51**, 739–742 (2013).

[38] Mikama, K., Daikuhara, H., Kasama, J., Yokoyama, A., Yokozawa, T. Synthesis of Poly(naphthalenecarboxamide)s with Low Polydispersity by Chain-Growth Condensation Polymerization *J. Polym. Sci.* A **49**, 3020-3029, (2011)

[39] A similar polymer was prepared in one previous report (reference 37). However, there, the monomer carried a longer solubilising side chain and only one polymer sample was reported which showed a narrower dispersity (D=1.11) after solvent extraction and/or HPLC purification.

[40] Sugi, R., Yokoyama, A., Furuyama, T., Uchiyama, M. & Yokozawa, T. Inductive Effect-Assisted Chain-Growth Polycondensation. Synthetic Development from para- to meta-Substituted Aromatic Polyamides with Low Polydispersities *J. Am. Chem. Soc*. **127**, 10172–10173 (2005).

[41] Ohishi, T., Sugi, R., Yokoyama, A. & Yokozawa, T. A variety of poly(m-benzamide)s with low polydispersities from inductive effect-assisted chain-growth polycondensation. *J Polym Sci Pol Chem*. **44**, 4990–5003 (2006).

[42] Hanselmann, R., Holter, D. & Frey, H. Hyperbranched Polymers Prepared via the Core-Dilution/Slow Addition Technique: Computer Simulation of Molecular Weight Distribution and Degree of Branching. *Macromolecules* **31**, 3790–3801 (1998).

[43] Sawamoto, M. & Kennedy, J. P. Quasiliving Carbocationic Polymerization. VI. Quasiliving Polymerization of Isobutyl Vinyl Ether. *Journal of Macromolecular Science: Part A - Chemistry* **A18**, 1275–1291 (1982).

[44] Sawamoto, M. & Kennedy, J. P. Quasiliving Carbocationic Polymerization. VIII. Quasiliving Polymerization of Methyl Vinyl Ether and Its Blocking from Quasiliving Poly(isobutyl Vinyl Ether) Dication. *Journal of Macromolecular Science: Part A - Chemistry* **A18**, 1301–1313 (1982).

[45] Urushibara, K. et al. Synthesis and Conformational Analysis of Alternately N-Alkylated Aromatic Amide Oligomers *J. Org. Chem*. **83**, 14338-14349, (2018).

[46] Gong, B. Hollow Crescents, Helices, and Macrocycles from Enforced Folding and Folding-Assisted Macrocyclization. *Accounts Chem. Res.* **41**, 1376–1386 (2008).

[47] König, H.M., Abbel, R., Schollmeyer, D., Kilbinger, A.F.M. Solid-Phase Synthesis of Oligo(*p*-benzamide) Foldamers *Org. Lett*. **8**, 1819-1822 (2006).

[48] Alizadeh, M. & Kilbinger, A. F. M. Synthesis of Telechelic Poly(p-benzamide)s *Macromolecules **51**,* 4363-4369 (2018).

[49] Orbelli Biroli, A. *et al.* Highly improved performance of ZnII tetraarylporphyrinates in DSSCs by the presence of octyloxy chains in the aryl rings *J. Mater. Chem. A* **3**, 2954-2959 (2015).

[50] Pal, S., Lucarini, F., Ruggi, A. & Kilbinger, A. F. M. Functional Metathesis Catalyst Through Ring Closing Enyne Metathesis: One Pot Protocol for Living Heterotelechelic Polymers *J. Am. Chem. Soc.* **140**, 3181-3185 (2018).

[51] Dolomanov, O. V., Bourhis, L. J., Gildea, R. J., Howard, J. A. K. & Puschmann, H. OLEX2: a complete structure solution, refinement and analysis program *J. Appl. Cryst.* **42**, 339-341 (2009).

[52] Sheldrick, G. M. SHELXT – Integrated space-group and crystal-structure determination *Acta Cryst. A* **71**, 3-8 (2015).

[53] Sheldrick, G.M. Crystal structure refinement with SHELXL *Acta Cryst. C* **71**, 3-8 (2015)

[54] Brandenburg, K. & Berndt, M. DIAMOND, Crystal Impact GbR, Bonn, Germany (1999).

[55] Markiewicz, P. & Goh, M. C. Simulation of atomic force microscope tip–sample/sample–tip reconstruction *J. Vac. Sci Technol. B* **13**, 1115-1118 (1995).

[56] Sader, J. E., Chon, J. W. & Mulvaney, P. Calibration of rectangular atomic force microscope cantilevers *Rev. Sci. Instrum.* **70**, 3967-3969 (1999).

[57] Hutter, J. L. & Bechhoefer, J. Calibration of atomic-force microscope tips *Rev. Sci. Instrum.* **64**, 1868-1873 (1993).